

RESEARCH ARTICLE

Employing bioactive compounds derived from *Ipomoea obscura* (L.) to evaluate potential inhibitor for SARS-CoV-2 main protease and ACE2 protein

Saravana Prabha Poochi¹ | Muruges Easwaran² |
Balamuralikrishnan Balasubramanian³  | Mohan Anbuselvam⁴ | Arun Meyyazhagan^{5,6} |
Sungkwon Park³ | Haripriya Kuchi Bhotla⁷ | Jeeva Anbuselvam⁸ |
Vijaya Anand Arumugam⁹ | Sasikala Keshavarao¹⁰ |
Gopalakrishnan Velliyur Kanniyappan¹¹ | Manikantan Pappusamy⁶ | Tanushri Kaul²

¹ Department of Biochemistry and Bioinformatics, Karpagam Academy of Higher Education, Coimbatore 641021, India

² Nutritional Improvement of Crops, International Centre for Genetic Engineering and Biotechnology, New Delhi 110067, India

³ Department of Food Science and Biotechnology, College of Life Science, Sejong University, Seoul 05006, Republic of Korea

⁴ Department of Biotechnology, Selvamm College of Arts and Science, Namakkal 637003, India

⁵ Euroespes Biomedical Research Centre, International Centre of Neuroscience and Genomic Medicine, Corunna 15165, Spain

⁶ Department of Life Sciences, Christ (Deemed to be University), Bangalore 560029, India

⁷ Department of Medicine, Section of Internal and Cardiovascular Medicine, University of Perugia, Perugia, Italy

⁸ Department of Animal Science, Bharathidasan University, Tiruchirappalli 620024, India

⁹ Medical Genetics and Epigenetics Laboratory, Department of Human Genetics and Molecular Biology, Bharathiar University, Coimbatore, Tamil Nadu, India

¹⁰ Professor and Emeritus (Rtd.), Human Genetics Laboratory, Department of Zoology, School of Life Sciences, Bharathiar University, Coimbatore, Tamil Nadu 46, India

¹¹ Department of Chemistry, College of Natural and Computational Sciences, Aksum University, Ethiopia

Correspondence

Tanushri Kaul, Nutritional Improvement of Crops, International Centre for Genetic Engineering and Biotechnology, New Delhi 110067, India.

Email: tanushri@icgeb.res.in

Balamuralikrishnan Balasubramanian equally contributed as a first author.

Abstract

Angiotensin converting enzyme 2 (ACE2) and main protease (M^{Pro}) are significant target proteins, mainly involved in the attachment of viral genome to host cells and aid in replication of severe acute respiratory syndrome-coronaviruses or SARS-CoV genome. In the present study, we identified 11 potent bioactive compounds from ethanolic leaf extract of *Ipomoea obscura* (L.) by using GC-MS analysis. These potential bioactive compounds were considered for molecular docking studies against ACE2 and M^{Pro} target proteins to determine the antiviral effects against SARS-COV. Results exhibits that among 11 compounds from *I. obscura* (L.), urso-deoxycholic acid, demeclocycline, tetracycline, chlorotetracycline, and ethyl iso-allocholate had potential viral inhibitory activity. Hence, the present findings suggested that chemical constitution present in *I. obscura* (L.) will address inhibition of corona viral replication in host cells.

This is an open access article under the terms of the [Creative Commons Attribution](https://creativecommons.org/licenses/by/4.0/) License, which permits use, distribution and reproduction in any medium, provided the original work is properly cited.

© 2020 The Authors. *Food Frontiers* published by NCU, NWU, JSU, ZJU & FAFU and John Wiley & Sons Australia, Ltd

KEYWORDS

ADME, GC-MS, *Ipomoea Obscura* (L.), Molecular docking, SARS-CoV-2

1 | INTRODUCTION

Convolvulaceae is one of the biggest family of flowering plants and possesses many members with medicinal and economic benefits. It comprises of 59 genera and 1,600 species. This family is widely distributed in both tropical and moderate temperature regions. One of its members *Ipomoea obscura* (L.) is a little climbing plant with small heart-shaped leaves and sharp-edged apex (Aiping et al., 2020; Saravana Prabha et al., 2017). It is native to parts of Africa, Asia, and certain Pacific Islands. Corolla is comprised of five fully fused petals. Seeds and fruits have been used as a cleansing agent to reduce breathing difficulties, alleviate pain, and improve vision (Shahina, 1994). The phytochemical constituents of *I. obscura* promote anti-inflammatory activity, antioxidant activity, anticancer activity, and antimicrobial activity against certain microorganisms. Ayurveda has explored numerous medicinal properties of this plant against dysentery, ulcers, hemorrhoids, and swellings (Christophe & Pharm, 2002). This plant grows mainly on fences or low ground cover as substrate in disturbed areas.

Severe acute respiratory syndrome (SARS) is a perilous pulmonary infection triggered by single stranded (+) sense RNA virus. Coronaviruses (CoVs) are largest family of RNA viruses with size ranging from 60 to 140 nm. It is further classified into four genera as α , β , γ , and δ . SARS-CoV-2 falls under the genus of β coronavirus (Markus et al., 2019). The main pathways of COVID-19 infection in humans are through droplets, aerosols, feces, and mouth mucus membranes of infected person and cause adverse symptoms such as typical acute respiratory infection, cough, fever, myalgia, sneezing, acute kidney injury, fatigue, acute liver injury, diarrhea, a sore throat, breathing collapse, as well as vomiting (Anthony & Stanley, 2015). The genome of corona virus composed of nonstructural proteins, accessory proteins, and structural proteins. Structural proteins had four major parts: one is spike surface glycol protein (S), tiny envelope protein (E), matrix protein (M), and nucleocapsid protein. The corona virus protein is mainly responsible for entry of SARS-CoV-2 in to host cell (Yong & Edward, 2020). Angiotensin converting enzyme 2 (ACE2) is an integral membrane glycoprotein mainly present in kidney, endothelium, lungs, and heart. The receptor-binding domain (RBD) of spike protein includes important amino acids (L455, F486, Q493, S494, N501, and Y505) that were involved in interaction and communication of single stranded RNA coronavirus genome (Andersen, Rambaut, Lipkin, Holmes, & Garry, 2020; Yifei, 2020). So far, six RBD amino acids have shown best binding activities against ACE2 receptors and for determining the host tropism of SARS-CoV-like virus. The spike envelope glycoprotein interacts with cellular receptors ACE2 to initiate membrane fusion and viral replications after the proteolytic cleavage event. Subsequently, viral genome is released into the cytoplasm and replicated viral particles then ini-

tiate the viral replication and cause adverse effect on a host organism. By blocking the ACE2/SARS-CoV-2 interaction, we could cease the viral replication and multiplication. The ACE2 and spike glycol protein may be considered as the attractive drug target for the discovery and development of effective antiviral drug against the viral disease (Bui et al., 2020; Fatima & Florian, 2020; Othman et al., 2020). One of the best characterized drug targets among CoV is the main protease (M^{pro}). Besides the papain-like protease, this enzyme is necessarily aimed at the dispensation of polyproteins that endure translated since the viral RNA. Impeding the action of this enzyme would block viral replication. Subsequently, proteases reported from *Homo sapiens* do not cleave the functional site by hybrid analogues, which is yet to be discovered. (Fatima & Florian, 2020; Mothay & Ramesh, 2020; Macchiagodena, Pagliai, & Procacci, 2020; Nisha Muralidharan, Sakthivel, Velmurugan, & Michael Gromiha, 2020). At present, there are no effective inhibitors against the novel corona virus; therefore, developing protein-based inhibitors for corona virus may emerge as a prerequisite strategy for curbing this virus. Computational methodologies have become an essential tool for drug discovery programs for the identification to lead optimization and formulation. Approaches such as ligand or structural based in silico techniques are commonly used in many discovery efforts. Henceforth, present investigation is carried out to identify bioactive compounds from *I. obscura* (L) and examine its antiviral activity against COVID-19 by the in silico approach.

2 | MATERIALS AND METHODS

2.1 | Sample leaves collection and hydrodistillation

The healthy mature and fresh leaves of *I. obscura* (L.) Ker Gawl were collected from Madurai district of Tamil Nadu, India. Taxonomic survey was authenticated by Dr. G.V.S. Murthy, Botanical Survey of India, TNAU Campus, Coimbatore, India. The documented specimen was deposited at TNAU Botany laboratory and utilized for further investigation. All leaf samples were maintained in our laboratory at proper environmental conditions and further used for phytochemical analysis.

2.2 | Chemicals reagents and apparatus

All chemical reagents were purchased from Sigma-Aldrich and applied for analysis with no further purification. The major apparatus included a hydrodistillation apparatus, a polarimeter, a Jasco V630 spectrophotometer, and a gas chromatography-mass spectrometer (GC-MS).

2.3 | Ethanolic extract preparation

The fresh leaves of *I. obscura* (L.) were carefully washed in running tap water, shade dried for 1 week, and powdered in an electric mixer grinder. The powdered leaves were subjected to ethanol solvent extraction. In total 300 g of dried plant powder was extracted utilizing Soxhlet extraction with 1.5 L of ethanol in a random shaker for 72 h at room temperature. Solvent extract was then evaporated using a rotary evaporator. The dried extract was collected in airtight bottles and stored at 4°C for further studies.

2.4 | Phytochemical analysis

Based on the preliminary phytochemical screening, the ethanolic leaf extract of *I. obscura* (L.) was subjected to GC-MS analysis on a Perkin Elmer gas chromatograph Clarus 500 Perkin Elmer system comprising an AOC-20i auto sampler and a gas chromatograph interfaced to a mass spectrometer prepared with Elite 5MS (5% diphenyl/95% dimethyl polysiloxane) fused silica column (30 mm × 0.25 mm × 0.25 μm df) that operated in electron impact mode with an ionization energy at 70 eV. Helium gas (99.999%) was utilized as a carrier gas at a constant flow rate of 0.1 mL/min and volume of 2 L was analyzed. The injector temperature was maintained at constant 250°C. Compounds present in ethanolic leaf extract were detected and cross-checked by comparing their retention indices and mass spectra fragmentation patterns using stored database in a computer library and with published literature, NIST08s.LIB (Lafferly, 1989) and WILEY8.LIB (Stein, 1990).

2.5 | Molecular docking simulation

Molecular docking is a computational approach for scrutinizing the interaction between the therapeutic target and a small molecule. In this investigation we performed *in silico* docking by applying Glide 5.5 (Dik-Lung, Daniel, & Chung, 2011; Glide, 2009), against respiratory therapeutic target ACE2 exhibited in human and M^{Pro} in SARS-CoV-2. The *in silico* docking exploration involves five steps, which are as follows.

2.5.1 | Collection and preparation of therapeutic target proteins

PDB Protein retrieval: The therapeutic targets ACE2 (PDB: 6M0J) and M^{Pro} (PDB: 6LU7) were retrieved from PDB structure, which possessed a resolution value 2.16 and 2.45 Å, respectively (Jin et al., 2020; Lan et al., 2020). Target proteins were preprocessed such as refinement, assigning bond orders, treating metals, and treating disulfides, building missing heavy atoms, formal charges, adjusting bond orders, adding hydrogen atom, and undesirable water molecule using PP-wizard. The protein structure energy was minimized until root mean square deviation (RMSD) cutoff was touched 0.30 Å. The consolidated protein structure was subsequently taken into receptor grid generation panel for receptor lattice generation, as binding pocket

HIGHLIGHTS

- Identified the potential bioactive compounds from *Ipomoea obscura* (L.) leaf extract.
- Molecular docking studies against ACE2 and M^{Pro} in SARS-CoV genome.
- Observed urso-deoxycholic acid, demeclocycline, tetracycline, chlorotetracycline and ethyl iso-allocholate has potential viral inhibitory activity.
- Molecular interaction study claims that urso-deoxycholic acid competitively binds with hACE2 and M^{Pro}.

information plays an important role in structure-based drug designing. The binding pocket residues were gathered from the literature. The residues like PHE 140, GLY 143, CYS 145, HIS 163, HIS 164, GLU 166, GLY 189, and THR 190 were mainly responsible for the protein-ligand interaction for M^{Pro} and ACE2. The grid package was generated by selecting the centroid of the chosen residues (20 Å × 20 Å × 20 Å), and then the grid constructed file was further used as input file for molecular docking studies.

2.5.2 | Preparation of *I. obscura* (L.) chemical constitution

Eleven bioactive compounds from medicinal plant *I. obscura* (L.) were identified. The ligands were subjected into Ligprep to optimize low-energy, three-dimensional (3D) structure with proper chiralities for each molecular arrangement. It generated various structure isolated molecules with ionization states, tautomers, stereo chemistries, and ring conformations. The force field was optimized by OPLS3.

2.5.3 | *In silico* docking into therapeutic

Glide is a popular and reliable tool for docking investigations, and here we employed glide version 5.5 performing for docking studies. The refined target protein structure (PDB ID: 6LU7, 6M0J) was utilized as the receptor, and prepared bioactive compounds from medicinal plant *I. obscura* (L.) were docked with an active site of target proteins by the Glide XP model (Schrodinger, 2009). We analyzed the protein-ligand interactions, glide score, and energy by a Glide XP visualizer.

2.6 | ADME properties assessment

Nowadays a failure rate of drug candidate increases in clinical stages due to undesired pharmacokinetics properties. The Absorption, Distribution, Metabolism, and Excretion (ADME) properties evaluation plays an important role in drug discovery. However, determination of

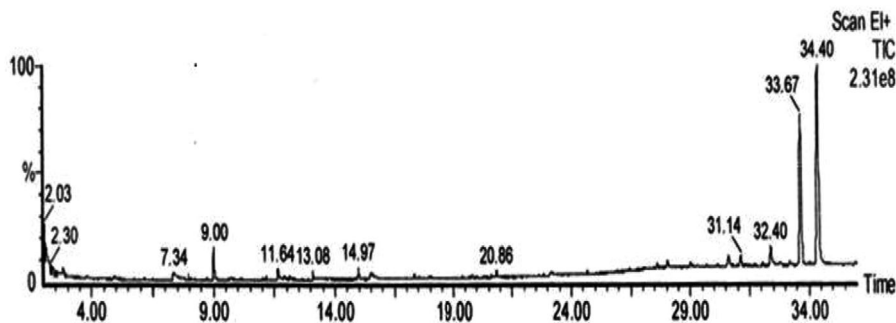


FIGURE 1 Gas-chromatogram of ethanolic leaf extract of *I. obscura* (L.)

TABLE 1 GC-MS spectral analysis of ethanolic leaf extract of *I. obscura* (L.)

S. No.	Retention time	Name of the compound	Molecular formula	Molecular weight	Peak (%)
1	2.30	Heptadecane, 9-hexyl-	C ₂₃ H ₄₈	324	7.30
2	7.34	Octadecane, 3-ethyl-5-(2-ethylbutyl)-	C ₂₆ H ₅₄	366	4.51
3	9.00	Oleic acid	C ₃₉ H ₇₆ O ₃	592	15.5
4	11.64	Tetracycline	C ₂₂ H ₂₄ N ₂ O ₈	444	5.13
5	13.08	Ursodeoxycholic acid	C ₂₄ H ₄₀ O ₄	392	3.23
6	14.97	Ethyl iso-allocholate	C ₂₆ H ₄₄ O ₅	436	3.54
7	20.86	Cholortetracycline	C ₂₂ H ₂₃ ClN ₂ O ₈	478	4.15
8	31.14	Cholestane-3,5-dichloro-6-nitro	C ₂₇ H ₄₅ Cl ₂ NO ₂	485	11.08
9	32.40	Demeclocycline	C ₂₁ H ₂₁ ClN ₂ O ₈	464	17.53
10	33.67	2-Cholestanone, 3-phenyl-	C ₃₃ H ₅₀ O	462	76.15
11	34.40	Lycopene	C ₄₀ H ₅₆	536	92.08

ADME experimentally is time consuming and expensive process. Thus, most of the pharmaceutical companies spend more amount on increasing the success rate of drug candidate/s. Interestingly, pharmaceutical companies and research groups mainly depend upon computational approach for ADME calculation. Qikprop has been employed to evaluate the drug-like properties of candidates (Lipinski, Lombardo, Dominy, & Feeney, 1997; QikProp, 2010) for instance, coefficient (QPlogP octanol/water), the water solubility (QPlogS), Lipinski's rule of five, gut blood-brain barrier (QPPCaco2), number of rotatable bonds, hydrophilic component of SASA, log IC50 value for blockage of K⁺ channels (QPlogHERG), percentage of human cell oral absorption, log P (water/gas), molecular weight, hydrogen bond donor, and hydrogen bond acceptor, which have been profiled for pharmacokinetics properties (Duffy & Jorgensen, 2009).

3 | RESULTS AND DISCUSSION

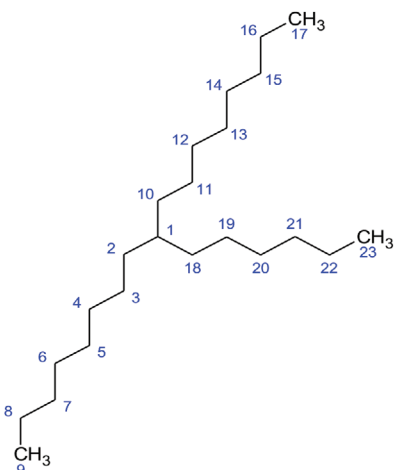
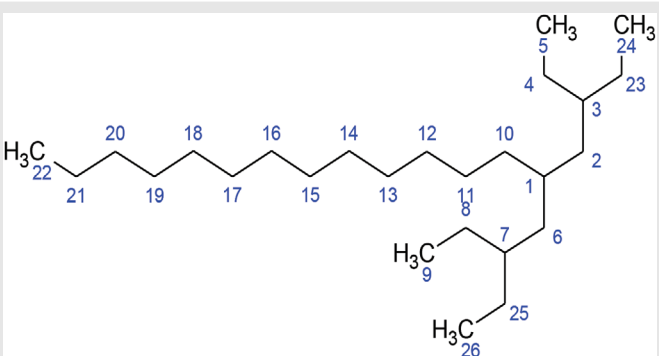
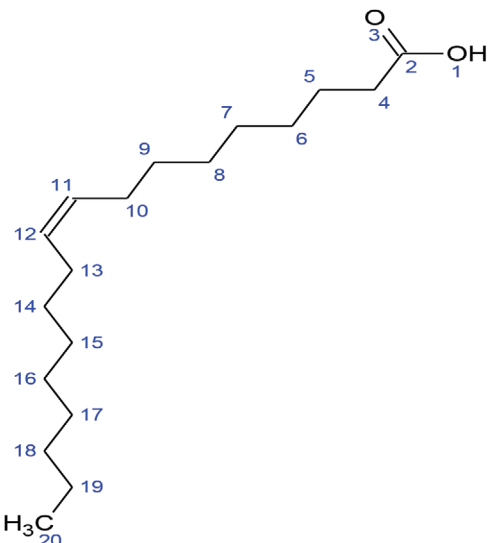
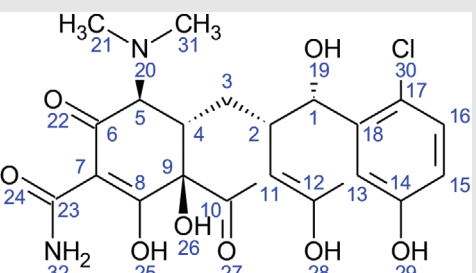
The GC-MS is extensively used in medical, pharmaceutical, environmental, and forensic applications, comprising of two analytical techniques with single methodology for investigating a mixture of chemical compounds present in extract (Casuga, Agnes, & Corpuz,

2016; Rao, Asheervadam, Khalilullah, & Murti, 1989). The components present in ethanolic leaf extract of *I. obscura* (L.) were identified, and their obtained chromatogram is shown in Figure 1. Active principles with their retention time molecular formula, molecular weight (MW), and percentage composition in ethanolic leaf extract of *I. obscura* (L.) had been identified. Compound prediction was based on the NIST library such as lycopene (92.08%), 2-cholestanone, 3-phenyl- (76.15%), demeclocycline (17.53%), oleic acid (15.5%), cholestane-3,5-dichloro-6-nitro (11.08%), heptadecane, 9-hexyl (7.30%), tetracycline (5.13%), octadecane, 3-ethyl-5-(2-ethylbutyl) (4.51%), cholortetracycline (4.15%), ethyl iso-allocholate (3.54%), urso-deoxycholic acid (3.23%) (see Tables 1 and 2).

3.1 | Docking simulation results of compounds present in *I. obscura* (L.) with ACE2 protein and M^{Pro}

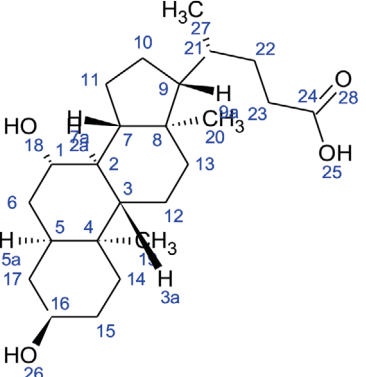
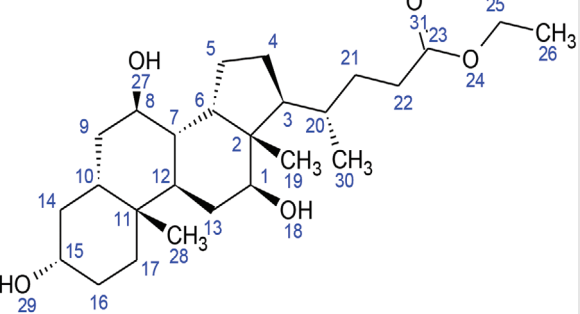
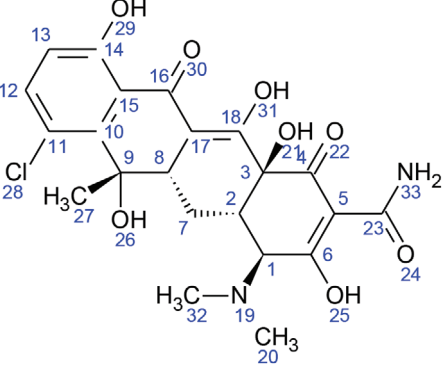
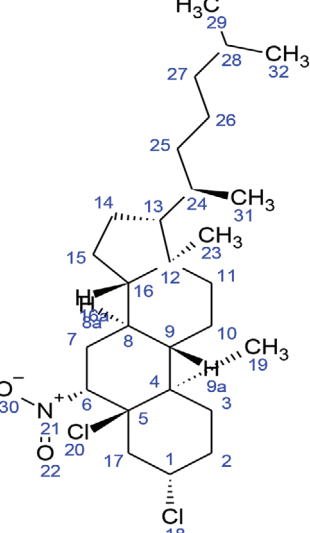
Interaction exposed that the key residues SER 511, TYR 196, GLN 102, and GLU 208 involved in hydrogen bond interacting ACE2 with the bond distance of 2.03, 1.66, 2.46, 1.94, and 1.95 Å, respectively. TRP 203, TYR 202, ALA 99, TYR 510, and LEU 95 residues participated in hydrophobic interaction. The glide score -7.739 kcal/mol

TABLE 2 Two-dimensional chemical structures of the 11 bioactive compounds from *I. Obscura* (L.)

No	Name of the compound	Molecular formula
1	Heptadecane, 9-hexyl-	
2	Octadecane, 3-ethyl-5-(2-ethylbutyl)-	
3	Oleic acid	
4	Tetracycline	

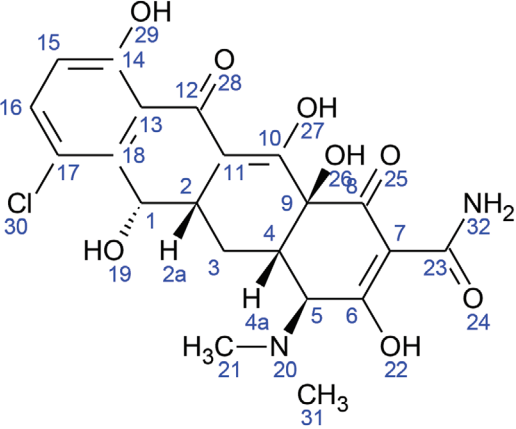
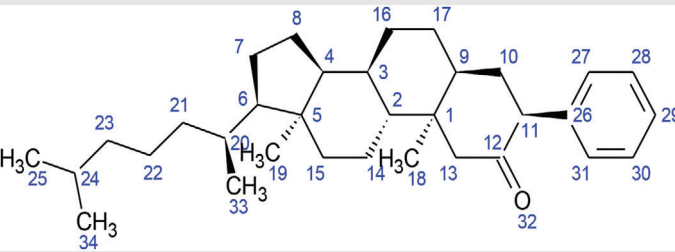
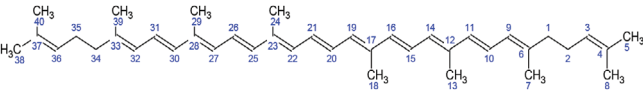
(Continues)

TABLE 2 (Continued)

No	Name of the compound	Molecular formula
5	Ursodeoxycholic acid	 <p>The structure shows a five-ring steroid nucleus with a hydroxyl group at C-3, a methyl group at C-10, and a propionic acid side chain at C-13. The side chain is numbered 21-25, with the methyl group at C-21 being 27. The hydroxyl group at C-24 is 25, and the carbonyl oxygen is 28.</p>
6	Ethyl iso-allochololate	 <p>The structure shows a five-ring steroid nucleus with hydroxyl groups at C-3 and C-12, and methyl groups at C-10, C-13, and C-14. A side chain at C-13 includes an ester linkage to an ethyl group. The ester oxygen is 23, the ethyl group is 25-26, and the carbonyl oxygen is 31.</p>
7	Cholortetracycline	 <p>The structure shows a tetracycline core with a chlorine atom at C-11, a methyl group at C-13, and a dimethylamino group at C-4. It has multiple hydroxyl groups at C-5, C-7, C-12, and C-14. The amino group is numbered 33, and the methyl groups on the nitrogen are 19 and 32.</p>
8	Cholestane-3,5-dichloro-6-nitro	 <p>The structure shows a five-ring steroid nucleus with a nitro group at C-6, chlorine atoms at C-3 and C-5, and a side chain at C-13. The side chain includes a methyl group at C-14 (31) and a methyl group at C-15 (32). The nitro group is numbered 20-22, and the chlorine atoms are 18 and 21.</p>

(Continues)

TABLE 2 (Continued)

No	Name of the compound	Molecular formula
9	Demeclocycline	
10	2-Cholestanone,3-phenyl-	
11	Lycopene	

and glide energy -48.990 kcal/mol were computed and are shown in Table 3 and Figure 2. The 6LU7 is the M^{PRO} found in the CoV associated with SARS and emerged as a potential drug target for COVID-19 (Khan, Khan, Khan, Ahmad, & Ansari, 2020). Initially, we observed reference molecule N3 glide score and glide energy -6.633 kcal/mol and -82.592 kcal/mol, respectively. The following residues ASP 287, HIS 41, and GLU 166 held on hydrogen bond interacting M^{PRO} with a bond length 2.27, 2.26, 2.22, and 2.10 Å and the following residues MET 49, CYS 44, VAL 186, CYC 145, PHE 181, LEU 141, TYR 54, and LEU 141 were involved in hydrophobic interaction with M^{PRO}. The urso-deoxycholic acid had two hydrogen bond interactions with M^{PRO}. Backbone oxygen atoms in PHE 140 interact with the hydrogen atom of urso-deoxycholic, and the hydrogen atom of urso-deoxycholic interacts with a side chain oxygen atom of SER 46 with a bond length (2.30, 1.93 Å). MET 49, MET 165, CYS 145, and LEU 141 participated in the hydrophobic interaction that enhanced stability of the protein-ligand complex as shown in Figure 3. The glide score -7.111 kcal/mol and glide energy -46.632 kcal/mol were calculated (see Table 4).

3.2 | ADME properties prediction

The bioactive compounds were further assessed for their drug-like behavior of ADME by use of QikProp. For the five bioactive molecules,

the aqueous solubility (QPlogS) necessary for absorption and delivery of drug inside the human body range between -5.766 and -2.623 , respectively. The percentage of human oral absorption for the bioactive compounds ranged from 23% to 95%. The predicted value of binding to human serum albumin (QPksha) fitted well within the acceptable range (~ -0.637 to -0.060). The predicted blood/brain barriers were within the acceptable range (~ -2.242 to -1.357). All the ADME properties are in adequate quality for solubility and permeability of cell membrane (Table 5): S in mol/L (acceptable range -6.5 to 0.5); percentage of human oral absorption ($<25\%$ is poor and $>80\%$ is high); prediction of binding to human serum albumin (acceptable range -1.0 to 1.5); prediction of brain/blood (acceptable range -3.0 to 1.2); the predicted rotatable bonds fit well with acceptable range 6–8; the predicted hydrophilic surface accessible solvent area (SASA) is under an acceptable range 158.858–314.842; molecular weight (<500 Da); hydrogen bond donor (<5); hydrogen bond acceptor (<10); predicted octanol/water partition coefficient $\log p$ (acceptable range -2.0 to 6.5).

3.3 | Molecular dynamics trajectory analysis

The RMSD and RMSF graphs for ACE2 versus urso-deoxycholic and M^{PRO} versus urso-deoxycholic are plotted in Figures 4 and 5. The M^{PRO}-urso-deoxycholic showed slight fluctuations at 5 than the entire

TABLE 3 Glide extraprecision (XP) results between molecular docking of five hit molecules and ACE2 using Schrodinger 10.2

S.No	Compound name	Glide score	Glide energy	Number of hydrogen bonds	Interaction residues	Distance (Å)
1	Urso-deoxycholic Acid	-7.739	-48.990	5	SER 511	2.03
					TYR 196	1.66
					GLN 102	2.46
					GLU 208	1.94, 1.95
2	Demeclocycline	-6.814	-62.708	7	ASP 206 (2)	1.99, 2.01
					TYR 202	2.46
					SER511 (2)	2.03, 1.95
					TRP 203	1.88
					LYS 562	2.42
3	Tetracycline	-5.809	-54.607	5	GLU 564	2.34,
					LYS 562,	2.36,
					GLN 98	2.08,
					GLU 208	1.70,
					TYR196	1.94
4	Chlorotetracycline	-5.405	-51.811	3	GLN 102	1.92
					LYS 562	2.09
					GLU 395	2.01
5	Ethyl iso-allocholate	-4.818	-43.927	5	ASP 509	2.05
					TRP 203	2.15
					TYR 202	2.01
					ASP 206	1.75
					LYS 562	2.02

TABLE 4 Glide extraprecision (XP) results between molecular docking of five hit molecules and M^{Pro} using Schrodinger 10.2

S.No	Compound name	Glide score	Glide energy	Number of hydrogen bonds	Interaction residues	Distance (Å)
1	Urso-deoxycholic acid	-7.11	-46.632	2	SER 46	1.93
					PHE 140	2.30
2	Demeclocycline	-6.807	-53.654	2	GLU 143	2.12
					GLU 166	2.25
3	Tetracycline	-5.949	-56.658	3	GLU 166 (2)	1.76
						2.14
4	Chlorotetracycline	-4.718	-40.084	6	THR 26 (2)	1.93
					GLU 143 (2)	2.20
					SER 144	2.33
					LEU 141	2.39
5	Ethyl iso-allocholate	-4.416	-43.229	2	THR 26	2.03
					GLU 189	1.89

simulation time. Initially, the RMSD of the main protease slightly fluctuated, the residues 48–138 were more stable, then slight fluctuation occurred between residues 139–143, and remaining residues were more stable during the entire simulation. The RMSD of the

ACE2 showed slight changes in starting time of simulation and reached maximum 3.5 Å, but some fluctuations or changes occurred between the residues 38 and 58. This molecular dynamic study suggested that the complex of SARS CoV-2 and ACE2-ursodeoxycholic

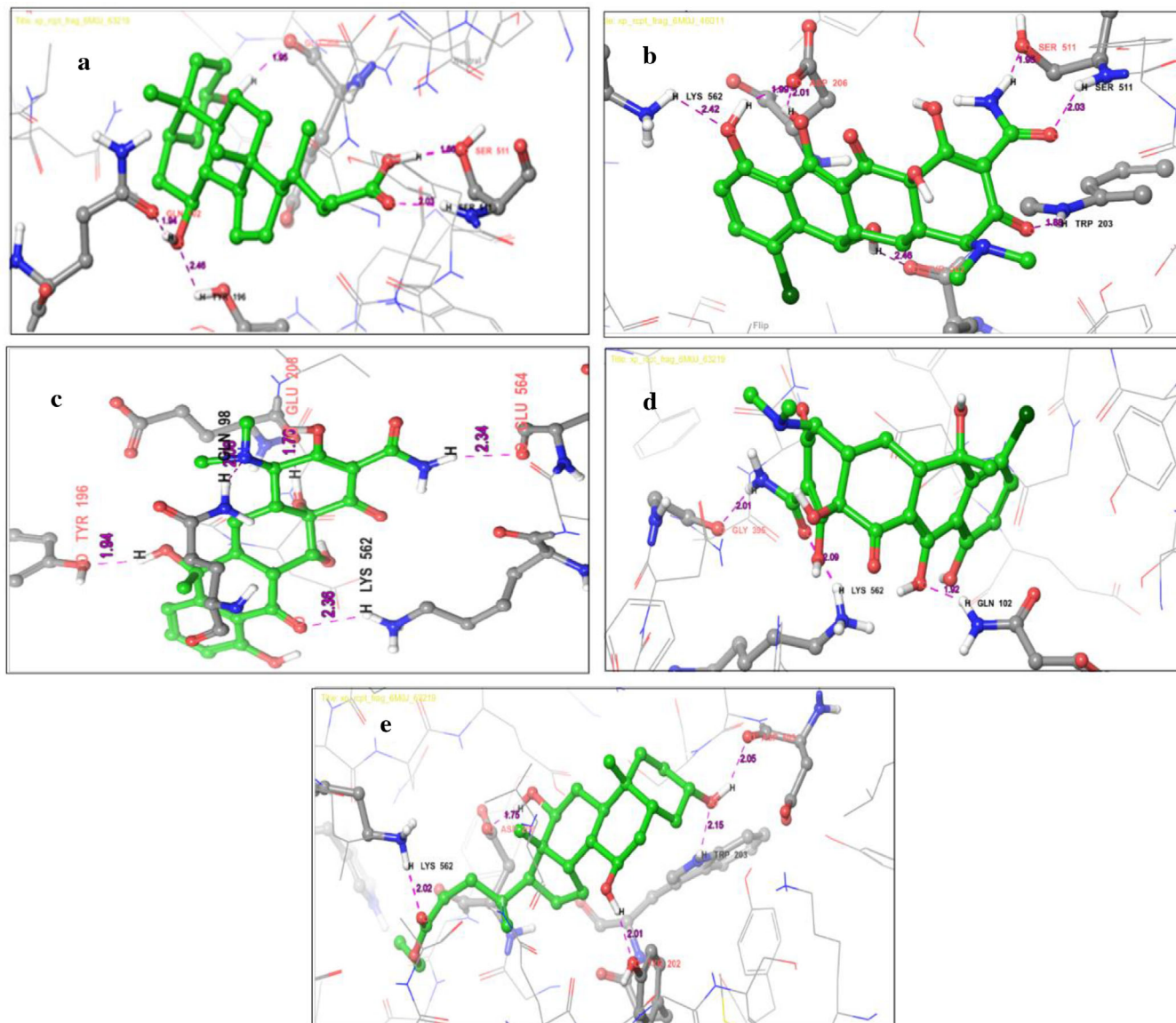


FIGURE 2 Two-dimensional interaction representation of the top five hit compounds in the active site of the ACE2: (a) urso-deoxycholic acid, (b) demeclocycline, (c) tetracycline, (d) chlorotetracycline, and (e) ethyl iso-allocholate

acids was more stable and produced increasingly reliable binding capabilities.

4 | CONCLUSION

Medicinal value of plants offers protection and cure to human beings from various life-threatening diseases. The existence of various bioactive compounds presents in plants provides evidence for the effective use against various ailments by conventional specialists. In the present work, phytochemicals were obtained from the leaf extract of *I. obscura* (L.) by GC-MS analysis. It is noteworthy that the chemical compounds of *I. obscura* can inhibit the ACE2 protein and M^{Pro} to block the viral receptivity. The molecular interaction study claims that urso-deoxycholic acid from *I. obscura* (L.) efficiently binds with ACE2 and

M^{Pro}. Further, *in vivo* and *in vitro* methods are consequently recommended to explicate the molecular mechanism, toxicity of the active constituents, side effects, circulating level, and pharmacokinetic properties of urso-deoxycholic acid to develop it as a potent drug against COVID-19.

ACKNOWLEDGMENTS

The authors thank ICGB authorities especially to the Director ICGB, New Delhi for providing the necessary infrastructure and ICGB core funds for this research work and to analyze and screen the molecules for COVID19 disease from our species of interest. We also thank Director General, ICGB Trieste, Italy and Department of Biotechnology (DBT) for financially supporting the research activities at ICGB. We thank the authorities of Karpagam Academy

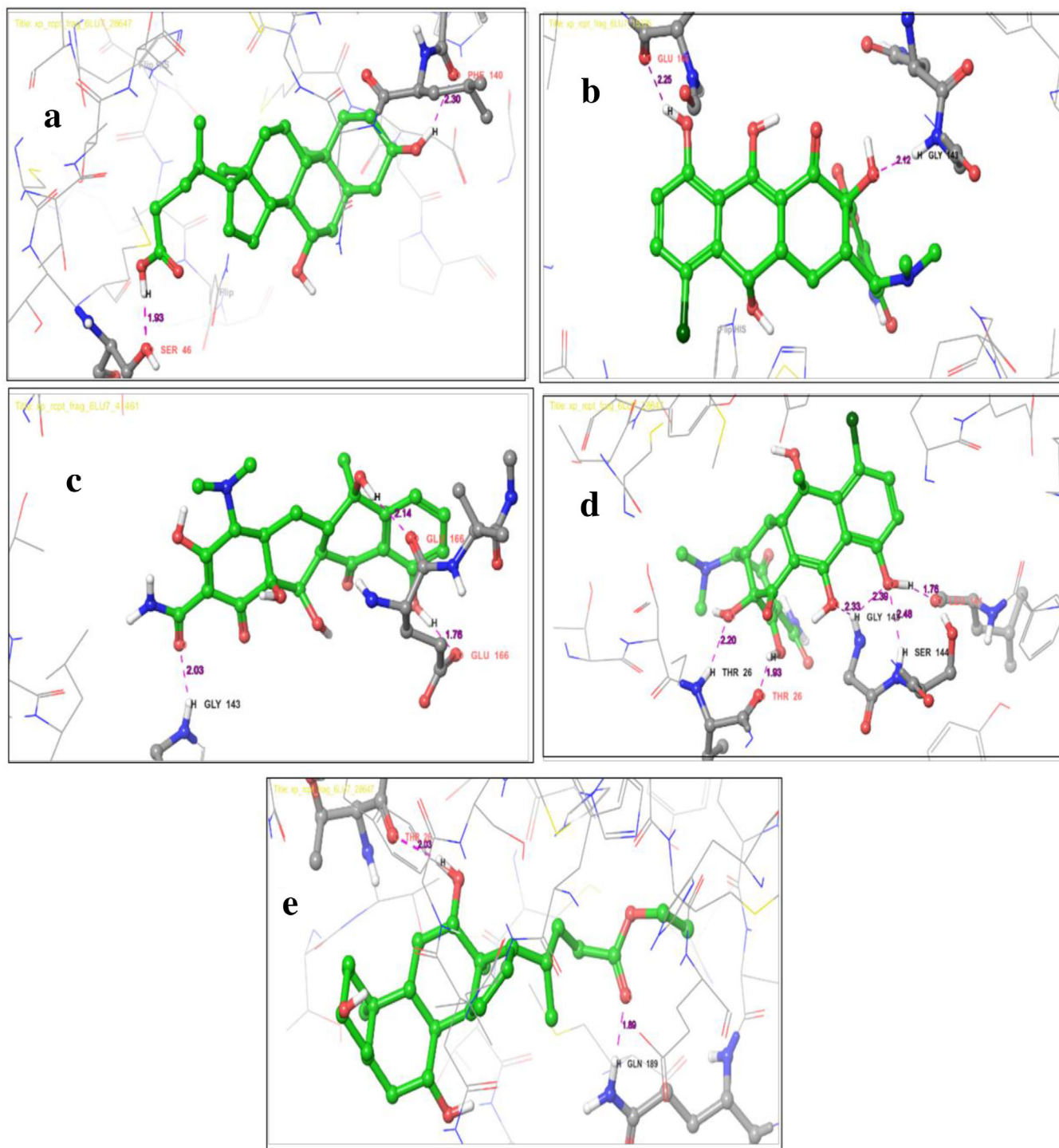


FIGURE 3 Three-dimensional interaction representation of the top five hit compounds in the active site of the SARS-CoV-2 M^{Pro}: (a) urso-deoxycholic acid, (b) demeclocycline, (c) tetracycline, (d) chlorotetracycline, (e) Ethyl iso-allocholate

of Higher Education for the facilities to carry out GC-MS analysis for our desired medicinal plants for the above-mentioned research work.

CONFLICT OF INTEREST

The authors declare no competing financial interest.

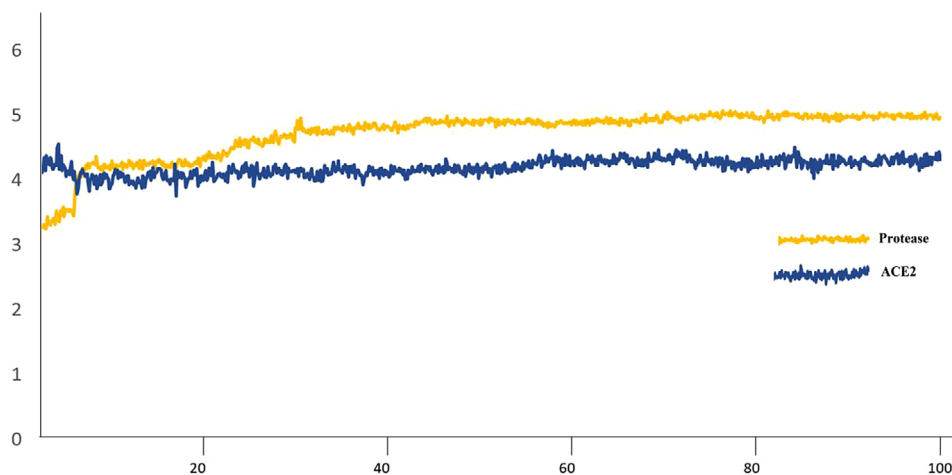
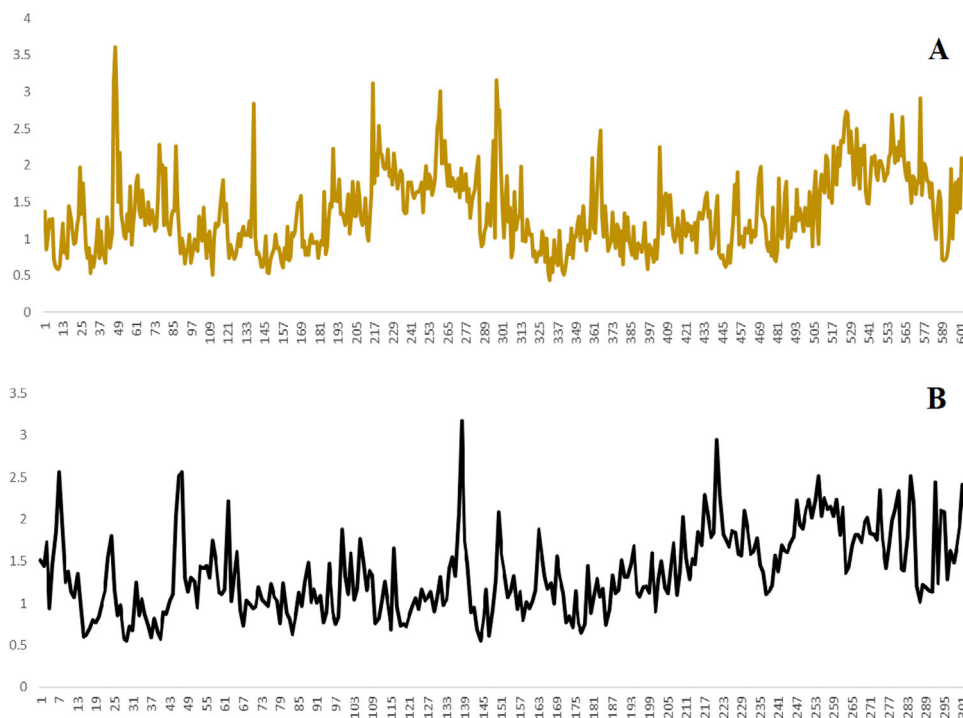
AUTHORS CONTRIBUTION

TK, EM, MA, and BB conceived and designed the experiments and wrote the paper. PSP, AM, AJ, and KBH contributed reagents and materials, performed the experiments, analyzed and interpreted the data, and wrote the paper. PS, AVA, KS, and VKG analyzed and interpreted the data and wrote the paper.

TABLE 5 Predicted aqueous solubility

Ligand ID	Hydrophilic SASA	RB	QPlogS	Percent human oral absorption	QPlogKhsa	log BB	Molecular weight	HBD	HBA	QPlog (o/w)
Ursodeoxycholic acid	189.129	6	-4.96	81	0.44	-1.35	392.5	3	5.40	3.84
Demeclocyclin	314.842	7	-2.67	24	-0.27	-2.17	464.8	4	10.2	0.09
Tetracycline	298.331	7	-2.62	23	-0.12	-2.24	446.4	3	9.20	0.06
Chlorotetracycline	280.885	7	-2.84	27	-0.06	-1.90	478.8	4	9.25	0.06
Ethyl iso allocholate	158.858	8	-5.76	95	0.63	-1.43	436.6	3	7.10	3.82

RB, Rotatable Bond; BB, Blood Brain Barrier; HBD, Hydrogen Bond Donor; HBA, Hydrogen Bond Acceptor.

**FIGURE 4** RMSD graph of SARS-CoV-2 M^{Pro} and ACE2-Urso-deoxycholic acid for the 100-ns simulation time**FIGURE 5** RMSF graph of SARS-CoV-2 M^{Pro} (a) ACE2 and (b) urso-deoxycholic acid for the 100-ns simulation time

ORCID

Balamuralikrishnan Balasubramanian  <https://orcid.org/0000-0001-6938-1495>

REFERENCES

- Aiping, W., Yousong, P., Baoying, H., Xiao, D., Xianyue, W. P. N., Jing, M., ... Taijjiao, J., (2020). Genome composition and divergence of the novel coronavirus (2019-nCoV) originating in China. *Cell Host Microbe*, 27, 325–328.
- Andersen, K. G., Rambaut, A., Lipkin, W. I., Holmes, E. C., & Garry, R. F., (2020). The proximal origin of SARS-CoV-2. *Nature Medicine*, 26, 450–452.
- Anthony, R. F., & Stanley, P. (2015). Coronaviruses: An overview of their replication and pathogenesis. *Methods in Molecular Biology*, 1282, 1–23.
- Bui, T. P. T., Tran, T. A. M., Nguyen, T. T. H., Le, T. H., Tran, T. H., Huynh, T. P. L., ... Nguyen, T. A. N. (2020). Investigation into SARS-CoV-2 resistance of compounds in garlic essential oil. *ACS Omega*, 5(14), 8312–8320.
- Casuga, F. P., Agnes, L. C., & Corpuz, M. J. T. (2016). GC-MS analysis of bioactive compounds present in different extracts of an endemic plant *Broussonetia luzonica* (Blanco Moraceae) leaves. *Asian Pacific Journal of Tropical Biomedicine*, 6(11), 957–961.
- Christophe, W., & Pharm, D. (2002). *Ethno pharmacology of medicinal plants: Asia and the Pacific* (Vol. 1, p. 69). New York, NY: Humana Press.
- Dik-Lung, M., Daniel, S. C., & Chung, H. L. (2011). Molecular docking for virtual screening of natural product databases. *Chemical Science*, 2, 1656–1665.
- Duffy, E. M., & Jorgensen, W. L. (2009). Prediction of properties from simulations: Free energies of solvation in Hexa decane, octanol, and water. *Journal of American Chemical Society*, 122, 2878–2888.
- Fatima, A., & Florian, K., (2020). SARS-CoV-2 vaccines: status report. *Immunity*, 52(4), 583–589.
- Jin, Z., Du, X., Xu, Y., Deng, Y., Liu, M., Zhao, Y., ... Yang, H. (2020). Structure of M^{pro} from COVID-19 virus and discovery of its inhibitors. *Nature*, 582 (7811), 289–293.
- Khan, M. F., Khan, M. A., Khan, Z. A., Ahmad, T., & Ansari, W. A. (2020). Identification of dietary molecules as therapeutic agents to combat COVID-19 using molecular docking studies. *Computational Chemistry*. (1). <https://doi.org/10.21203/rs.3.rs-19560/v1>
- Lafferly, M. F. W. (1989). *Registry of mass spectral data*, 5th ed. New York: Wiley.
- Lan, J., Ge, J., Yu, J., Shan, S., Zhou, H., Fan, S., ... Wang, X. (2020). Structure of the SARS-CoV-2 spike receptor-binding domain bound to the ACE2 receptor. *Nature*, 581(7807), 215–220.
- Lipinski, C. A., Lombardo, F., Dominy, B. W., & Feeney, P. J. (1997). Experimental and computational approaches to estimate solubility and permeability in drug discovery and development settings. *Advanced Drug Delivery Reviews*, 23(1-3), 3–25.
- Markus, H., Hannah, K. W., Simon, S., Nadine, K., Tanja, H., Sandra, E., ... Stefan, P. (2019). SARS-CoV2 cell entry depends on ACE2 and TMPRSS2 and is blocked by a clinically proven protease inhibitor. *Cell*, 181, 1–10.
- Macchiagodena, M., Pagliai, M., & Procacci, P., (2020). Identification of potential binders of the main protease 3CL^{pro} of the COVID-19 via structure-based ligand design and molecular modeling. *Chemistry Physics Letters*, 750, 137489.
- Mothay, D., & Ramesh, K. V., (2020). Binding site analysis of potential protease inhibitors of COVID-19 using AutoDock. *Virusdisease*, 2, 1–6.
- Muralidharan, N., Sakthivel, R., Velmurugan, D., & Michael Gromiha, M., (2020). Computational studies of drug repurposing and synergism of lopinavir, oseltamivir and ritonavir binding with SARS-CoV-2 protease against COVID-19. *Journal of Biomolecular Structure Dynamics*. Advance online publication. <https://doi.org/10.1080/07391102.2020.1752802>
- Othman, H., Bouslama, Z., Brandenburg, J. T., da Rocha, J., Hamdi, Y., Ghedira, K., Srairi-Abid, N., & Hazelhurst, S. (2020). Interaction of the spike protein RBD from SARS-CoV-2 with ACE2: Similarity with SARS-CoV, hot-spot analysis and effect of the receptor polymorphism. *Biochemistry and Biophysics Research Communication*, 527(3), 702–708.
- QikProp. (2010). *QikProp*, version 2.3. New York, NY: Schrodinger LLC.
- Rao, P. S., Asheevadam, Y., Khalilullah, M., & Murti, V. V. S. (1989). A revised structure for the isoflavone lanceolarrin. *Phytochemistry*, 28, 957–958.
- Saravana Prabha, P., Krishna Chaithanya, K., Zenebe, H., Nagaraju, B., & Gopalakrishnan, V. K., (2017). Isolation and identification of bioactive compound from *Ipomoea obscura* (L.) ker gawl. *Journal of Pharmaceutical Research*, 11(1), 10–14.
- Schrodinger LLC. (2009). *Glide*, version 5.5. New York, NY: Author.
- Schrodinger LLC. (2009). *Protein preparation Wizard Maestro*. New York, NY: Author.
- Shahina, A. (1994). *Handbook of Arabian medicinal plants*. Boca Raton, FL: CRC Press, 90.
- Stein, S. E., (1990). *National Institute of Standards and Technology (NIST) Mass Spectral Database and Software*, Version 3.02. Gaithersburg, MD: NIST.
- Yong, Z. Z., & Edward, C. H. (2020). A genomic perspective on the origin and emergence of SARSCoV-2. *Cell*, 181(2), 1–5.
- Yifei, X., (2020). Unveiling the origin and transmission of 2019-nCoV. *Trends in Microbiology*, 28(4), 239–240.

How to cite this article: Balasubramanian B, Easwaran M, Poochi SP, et al. Employing bioactive compounds derived from *Ipomoea obscura* (L.) to evaluate potential inhibitor for SARS-CoV-2 main protease and ACE2 protein. *Food Frontiers*. 2020;1:168–179. <https://doi.org/10.1002/fft2.29>